

PAPER • OPEN ACCESS

## Electrochemical Disposition of Titanium Dioxide Photocatalyst on Micropores Silicon Wafer for Water Treatment Application

To cite this article: Esmail, A. M. Basheer *et al* 2020 *IOP Conf. Ser.: Mater. Sci. Eng.* **736** 042015

View the [article online](#) for updates and enhancements.

# Electrochemical Disposition of Titanium Dioxide Photocatalyst on Micropores Silicon Wafer for Water Treatment Application

Esmail. A. M. Basheer<sup>1</sup>, Wafaa K. Mahmood<sup>2</sup>, and Hayder A. Abdulbari<sup>3\*</sup>

<sup>1</sup>Faculty of Chemical & Natural Resources Engineering, Universiti Malaysia Pahang, Lebuhraya Tun Razak, 26300 Gambang, Kuantan, Pahang, Malaysia

<sup>2</sup>Department of Production Engineering and Metallurgy, University of Technology-Iraq, Baghdad, IRAQ

<sup>3</sup>Centre of Excellence for Advanced Research in Fluid Flow (CARIFF), Universiti Malaysia Pahang, Lebuhraya Tun Razak, 26300 Gambang, Kuantan, Pahang, Malaysia

\*E-mail: [hayder.bari@gmail.com](mailto:hayder.bari@gmail.com)

**Abstract.** Titanium dioxide (TiO<sub>2</sub>), due to wide band gap, has a limited use in water treatment process because of its low activity under visible light. Such drawback is usually associated with the inadequate solar spectrum that activates its surface, i.e., most of the photoexcited electron-hole pairs tend to recombine, leading to a reduction in the photocatalytic performance. Immobilization of TiO<sub>2</sub> on the surface of silicon is considered as a useful approach to overcome this drawback. However, the immobilization methods require high temperature and pressure, which limit the numbers and types of materials that can be utilized as a substrate. The known electrochemical deposition procedures are usually conducted through two major steps, electrochemical oxidation and hydrolysis of Ti(III) precursor to form a thin layer on the surface of the substrate, followed by thermal annealing to form crystalline phase. The present work introduces the immobilization of titanium dioxide on a microporous silicon (MPSi) wafer through direct electrochemical deposition, where titanium dioxide P25 was used in the electrolyte solution. The photocatalyst surface morphology and composition were characterized using Scan Electron Microscope (SEM), Electron Dispersive X-ray (EDX), X-ray diffraction (XRD), and X-ray Photoemission Spectroscopy (XPS) techniques. The photocatalytic activities of the new composites were investigated, and the experimental results indicate that the fabricated TiO<sub>2</sub>-MPSi showed higher methylene blue degradation rate than that of the conventional P25 catalyst. This is due to the unique photosensitivity and porous structure of the new photocatalytic composites. With the advantages of using this method, it is believed that more efficient photocatalyst can be produced.

## 1. Introduction

Titanium dioxide is one of the semiconductor oxides that has been studied extensively due to its unique properties such as high photocatalytic activity under UV light, good chemical and biological



stability, availability, and cost effective [1-4]. Nevertheless, a very limited applications that can utilize  $\text{TiO}_2$  as a photocatalyst due to the limited solar energy that can be used by the system [5]. This limitation is associated to the large band gap energy (3.2eV) of  $\text{TiO}_2$  which limits the solar spectrum that activates the surface to only the UV region which is a very small portion of the solar light (3.4% of the solar light) [6-8]. Additionally, most of the photoexcited electron-hole pairs tend to recombine in the  $\text{TiO}_2$  surface, leading to a reduction in the photocatalytic performance [9, 10]. To date, many approaches have been introduced to reduce the electron-hole recombination such as immobilizing  $\text{TiO}_2$  on activated carbon [11-13], graphene [14, 15], human hair [4], and silica gel [16]. To reduce the  $\text{TiO}_2$  band gap with the intention of improving the light absorption in the visible region, studies have been conducted involving disposition of  $\text{TiO}_2$  on the surface of metallic and nonmetallic materials [17, 18]. Several methods have been used successfully to deposit  $\text{TiO}_2$  thin films, including the sol-gel method [18], chemical vapor deposition (CVD) [19], physical vapor deposition (PVD) [20], chemical bath deposition (CBD) [21], and reactive sputtering and atomic layer deposition (ALD) [22]. Nevertheless, immobilizing titanium dioxide using these methods requires either high temperature or high pressure to achieve an acceptable coverage of the surface with titanium dioxide. The heating step is essential to form the crystalline phase, which defines the photocatalytic activity of the catalyst. For example, vapor or vacuum deposition techniques for preparing functional thin films typically undergoes a deposition of titanium-based clusters, followed by a thermal post-annealing process to crystallize the film. In addition, the crystalline phase obtained using these methods is of low intensities, which results in low photo activities. Titanium dioxide has been immobilized on the surface of some materials and has shown photocatalytic activity improvement due to the band gap narrowing. [17] presented the immobilization of  $\text{TiO}_2$  on the surface of  $\text{SiO}_2$  using atomic layer deposition (ALD). They reported that  $\text{TiO}_2$ -coated samples adsorbed more toluene than that of the bare silica under dry conditions. Another study showed a high performance of  $\text{TiO}_2$  doped on ZnO surface [23]. The composite photocatalyst has the advantage of utilizing a high ratio of light together with the low recombination rate of electron-hole pairs, due to the reduction of the band gap. To incorporate titanium dioxide with other materials under ambient conditions which can utilize visible light, a direct electrochemical disposition is believed to be a suitable approach.

In this work, a new composite of titanium dioxide photocatalyst was fabricated which can utilize visible light. Titanium dioxide was immobilized on the surface of microporous silicon wafer through direct electrochemical deposition. The immobilization and the performance of the titanium dioxide were investigated and compared to the sol-gel methods.

## 2. Materials and Method

### 2.1. Materials

A p-type silicon wafer, polyvinyl alcohol (PVA), acetic acid, ammonium fluoride ( $\text{NH}_4\text{F}$ ), 2-propanol, titanium nitrate [ $\text{Ti}(\text{NO}_3)_4$ ], absolute ethanol (99.99%), methylene blue, commercial titanium dioxide P25, and polyethylene glycol were purchased from Sigma-Aldrich Malaysia.

### 2.2. Experiments

*2.2.1. Fabrication of Microporous Silicon Wafer.* The electrochemical laser etching of the silicon was conducted using a simple electrochemical cell setup where the silicon wafer was used as cathode and platinum electrode as anode. The electrolyte used consisted of 48% (v/v) of  $\text{NH}_4\text{F}$  and ethanol. The electrochemical etching was assisted by illuminating green laser beam with a wavelength of 532 nm (the laser source was set up to be 4 cm from the silicon wafer surface). The etching process was fixed at 45 min

*2.2.2. Synthesis of TiO<sub>2</sub>-MPSi Composite by Sol-Gel Method.* TiO<sub>2</sub> was immobilized on the prepared microporous silicon wafer using the simple sol-gel method. In short, 2 g of TiO<sub>2</sub> (P25; 70% anatase and 30% rutile) were mixed with 5 g of PVA in 50 mL of 2-propanol and 50 mL of deionized (DI) water for 3 h. The mixture pH was adjusted to 5 by adding several drops of acetic acid. The mixture was heated up to 50 °C with stirring overnight. The obtained sol-gel was sonicated for 60 min to be ready for use. Prior to the coating, the silicon wafer was washed with nitric acid followed by rinsing with ethanol and DI water. The prepared sol-gel was deposited on the MPSi wafer using a spin coater (SCS) at 1200 rpm. The prepared TiO<sub>2</sub>-MPSi composites were annealed at 550 °C for 2 h at 3 °C/min.

*2.2.3. Synthesis of TiO<sub>2</sub>-MPSi Composite by Electrochemical Anodization.* The electrochemical deposition of TiO<sub>2</sub> on the surface of the prepared MPSi wafer was done using a simple electrochemical cell setup where the MPSi acted as anode and titanium mesh as cathode. The electrochemical deposition was carried out in Ti(NO<sub>3</sub>)<sub>4</sub> electrolyte mixed with 12 wt% of titanium dioxide (P25) powder, under 60 V for 60 min.

### 2.3. Photocatalytic Activity.

In a typical experimental run, 50 mL of 18 mM of methylene blue aqueous solution was placed in a reactor with 2 × 3 cm photocatalyst placed vertically at the centre. During the measurement of the photocatalytic performance, the size of photocatalyst was kept the same in all experiments. The solution was magnetically stirred in dark for 60 min to ensure the adsorption-desorption equilibrium. After the dark treatment, the solution was irradiated with xenon simulated solar light (125 W). The degraded MB solution was collected, and the concentration was determined by monitoring the change in characteristic absorption peak at λ = 664 nm using a UV-visible spectrophotometer. The fractional conversion was calculated as follows [4]:

$$\text{Conversion (\%)} = \frac{A_0 - A}{A_0} \times 100 \quad (1)$$

where A<sub>0</sub> is the initial absorbance value, and A is the absorbance value of the degraded solution.

## 3. Results and Discussion

Silicon is an outstanding conductive material with high photoactivities. The immobilization of titanium dioxide on the surface of silicon wafer is one of the most successful developed titanium photocatalyst composites due to the narrow band gap that silicon provides. However, the surface characteristics usually defines the ability of immobilization, where porosity is an important factor. Therefore, preparing the surface of silicon before deposition of titanium dioxide is an important step [24]. Figure 1 shows the surface of the silicon wafer before and after the electrochemical etching assisted with laser projection. As shown in Figure 1a, a flat surface with very low porosity was observed and some non-uniform cracks can be noticed on the surface. This is considered as one of the disadvantages of silicon on photoactivity application, because it causes high reflection of the spectra when placed under light sources. The electrochemical etching surface treatment assisted with laser projection resulted in high porosity and uniform shape as shown in Figure 1b. Fundamentally, etching process starts with the replacement of superficial hydrogen atoms (H<sup>+</sup>) by fluoride ions (F<sup>-</sup>) which are incorporated from the etching electrolyte solution. This step creates an electronic hole (h<sup>+</sup>), which promotes the formation of F-Si bond under the anodic bias by the polarization effect induced by the F atom over the Si atom. Accordingly, this mechanism is repeated to weaken the Si-Si bond. Finally, the Si atom etches away from the silicon wafer surface during the reaction and a porous structure is formed on the surface of the silicon wafer as represented in Equation 2 [24].

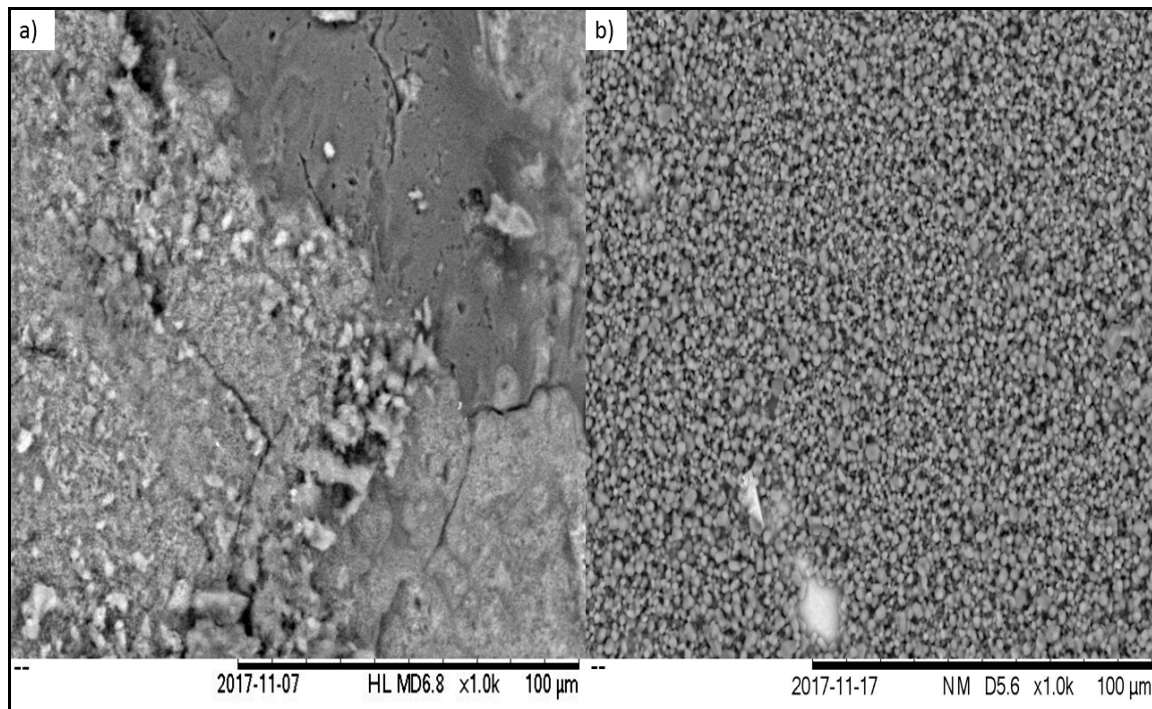
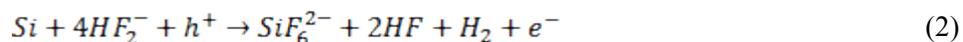


**Figure 1** SEM images of MPSi (a) before and (b) after etching



However, this mechanism in normal electrochemical might result in random distribution and non-uniform porous structure. The laser projection in this study assisted the etching in two ways, weakening the Si–Si bond and directed the pores uniformly. As shown in Figure 2, the whole surface of the silicon wafer was found to be porous. Figure 2a shows the microstructure of the silicon surface at 30  $\mu\text{m}$ , where the pores can be seen as hollow spots in the middle of the Si structure. The surface porosity can be clearly noticed even at low magnitude scanning of SEM, as evident of the deep etching that can be achieved with the laser projection. Projecting the laser usually initiates sites on the surface of silicon, which attract the fluoride etching at these sites. As the laser projected in specific areas, the etching will always take place in these areas, hence the etching can be controlled.

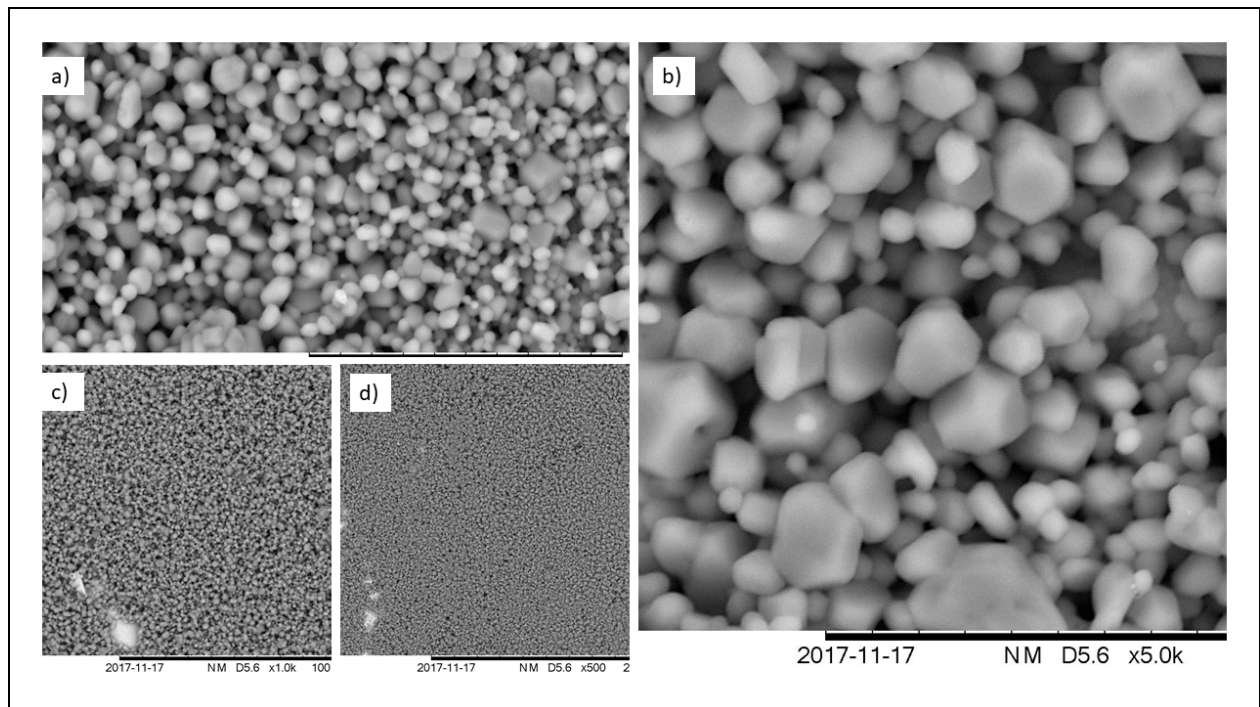


**Figure 2** SEM images of MPSi at (a) 30, (b) 20, (c) 100, and (d) 200  $\mu\text{m}$ .

The electrochemical deposition of titanium dioxide on the surface of silicon wafer took place after the preparation of the surface as described earlier. The morphologies of the as-prepared MPSi–TiO<sub>2</sub> composites after the disposition were characterized using SEM. The surface morphology of the composites can be described as coral reef shape. As shown in Figure 3a, the total coverage of the surface was not achieved. However, a significant amount of titanium dioxide was deposited on the surface of the silicon wafer.

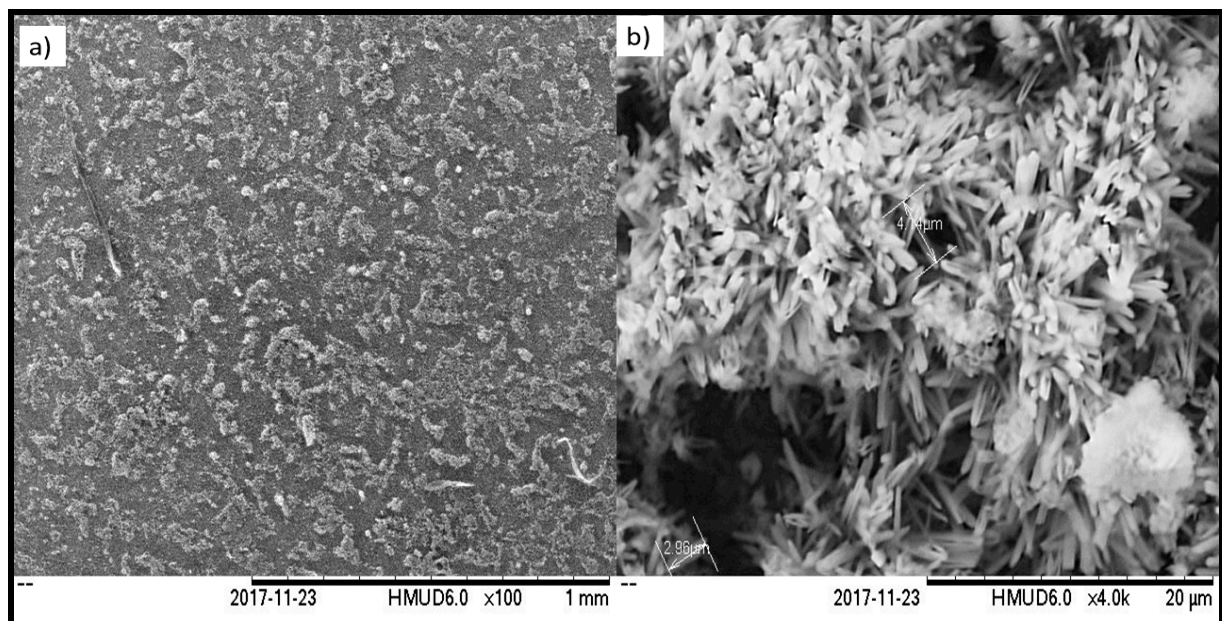


**Figure 3** SEM images of the MPSi–TiO<sub>2</sub> prepared via electrochemical deposition

Figure 4 shows the SEM images of the immobilized silicon surface obtained via electrochemical deposition and sol-gel methods. The electrochemical immobilization of titanium dioxide on the surface of the silicon wafer resulted in nanotubes growth. As shown in Figure 4a, the titanium dioxide immobilized on the surface was dense and penetrated into the inner surface of the silicon pores. The growth of titanium dioxide nanotubes intensively increased at the porous sites. In contrast, the sol-gel method resulted in less uniform distribution of titanium dioxide on the surface of silicon. Regardless of methods, the formed titanium dioxide layer thickness was more uniformed at all the sites and the surface coverage was low as described by the EDX results in Table 1. This is an advantage of using the sol-gel method, where the thickness of the titanium dioxide will depend mainly on the speed of the coater and time for coating. In other words, the desired thickness of deposited titanium dioxide can be achieved by controlling the coating variables (speed and time of the coating). As shown in Figure 2b, the titanium dioxide film on the surface of the silicon wafer covered the microporous structure of silicon, which lowered the ability of titanium to link to silicon. In contrast, the surface of silicon after the electrochemical disposition was found to be porous. This results in increasing contact between silicon and titanium dioxide film.

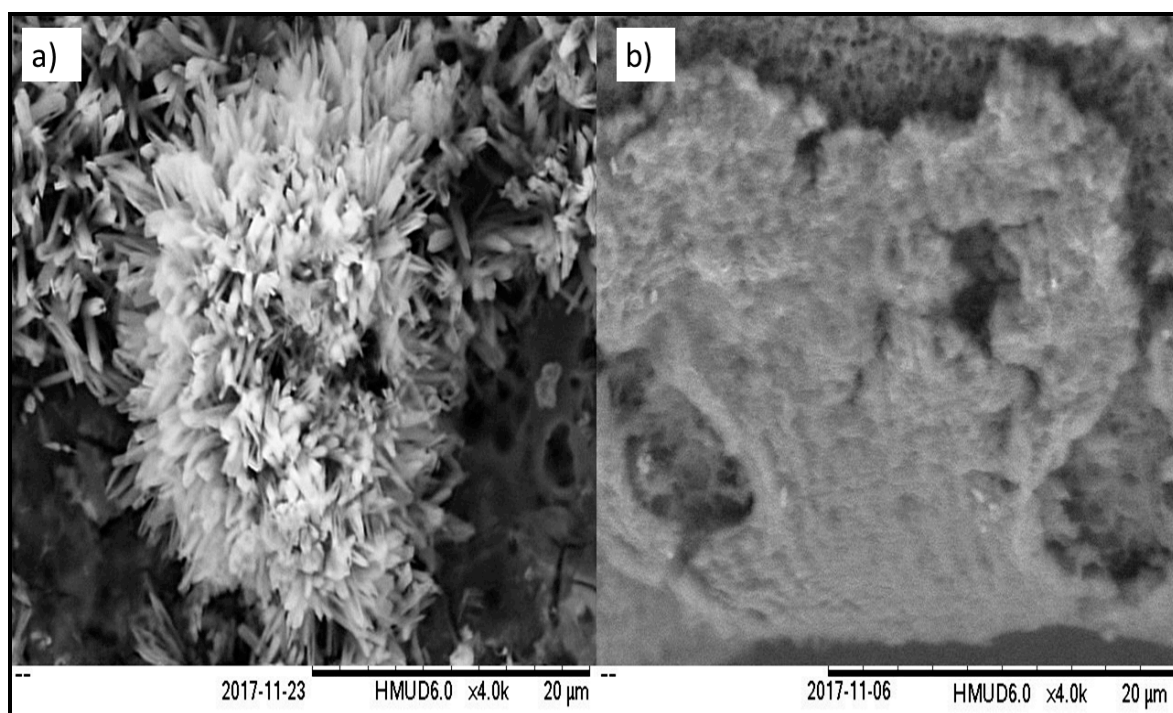


**Figure 4** SEM images of the MPSi/TiO<sub>2</sub> composites prepared via (a) electrochemical deposition and (b) sol-gel methods

Table 1 shows the amount of titanium dioxide obtained via each method. The sol-gel method produced a higher amount of titanium dioxide compared to that obtained via the electrochemical deposition, due to the ability to control the thickness of the film by controlling the coating variables such as speed and time of coating.

**Table 1** Titanium Dioxide amount in the prepared MPSi–TiO<sub>2</sub> composites obtained using EDX analysis

Method	Titanium Dioxide (wt.%)
Electrochemical Deposition	25.633
Sol–gel	36.084

Figure 5 shows the XRD pattern of the titanium dioxide prepared by the sol–gel and electrochemical deposition methods in comparison to the commercial TiO<sub>2</sub> (P25). The peaks at a  $2\theta$  value of  $25.6^\circ$  observed in the sample prepared using sol–gel method correspond to the crystal planes of titanium dioxide anatase phase (101). Similar peaks were observed for the prepared composite using electrochemical deposition. Nevertheless, the peak was found to be higher in the case of electrochemical deposition compared to that of the sol–gel method. This is due to the high intensity of the rutile phase obtained in the sol–gel method due to the high calcination temperature. Similar peaks were also observed at  $37.8^\circ$ ,  $48.0^\circ$ , and  $53.9^\circ$  which correspond to the (004), (200), and (105) crystal planes of the TiO<sub>2</sub> anatase phase, respectively. In addition, diffraction peaks were also observed at  $27.4^\circ$ ,  $36.1^\circ$ ,  $41.2^\circ$ , and  $56.7^\circ$ , which can be attributed to the (110), (101), (111), and (220) planes of the TiO<sub>2</sub> rutile phase, respectively. Based on these results, the rutile and anatase TiO<sub>2</sub> phases coexist in the TiO<sub>2</sub> nanoparticles deposited on the silicon substrate prepared by both methods. In comparison, anatase phase dominated in the prepared TiO<sub>2</sub> composite produced via the electrochemical disposition.

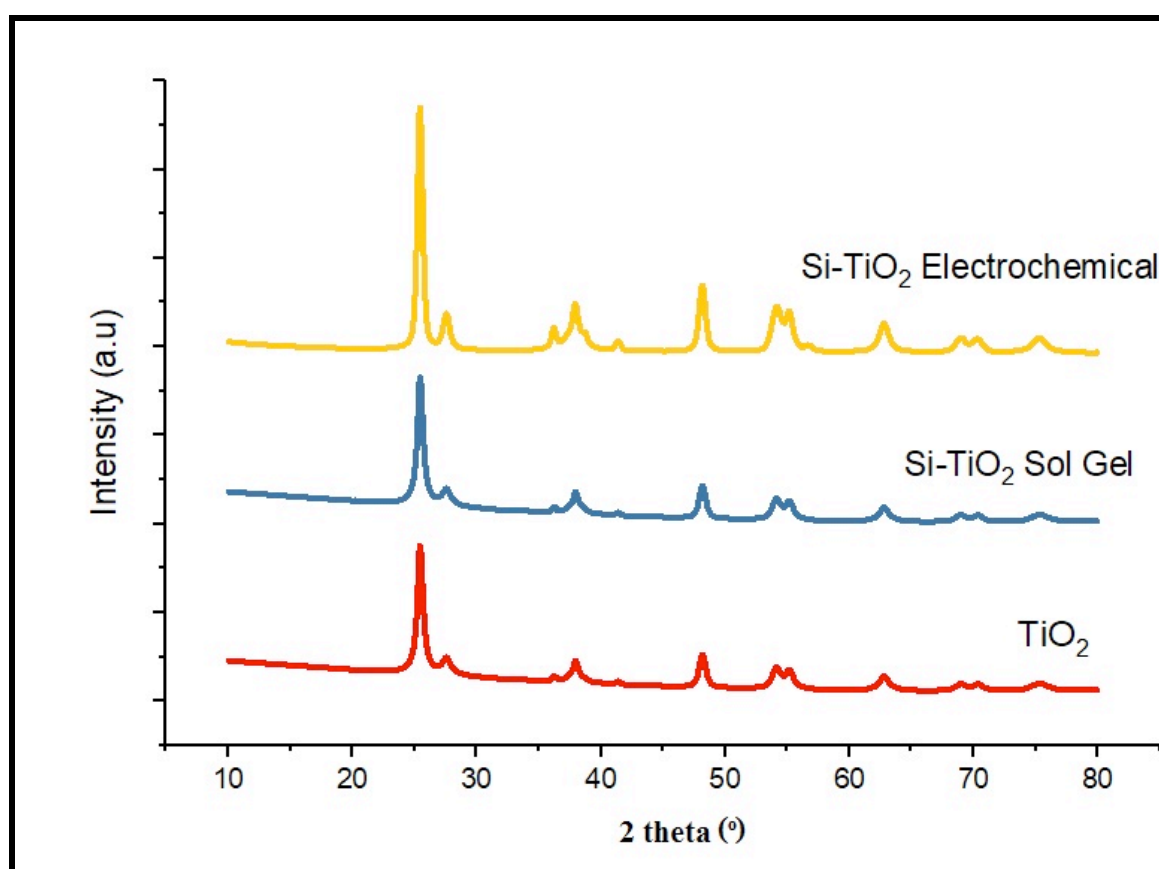
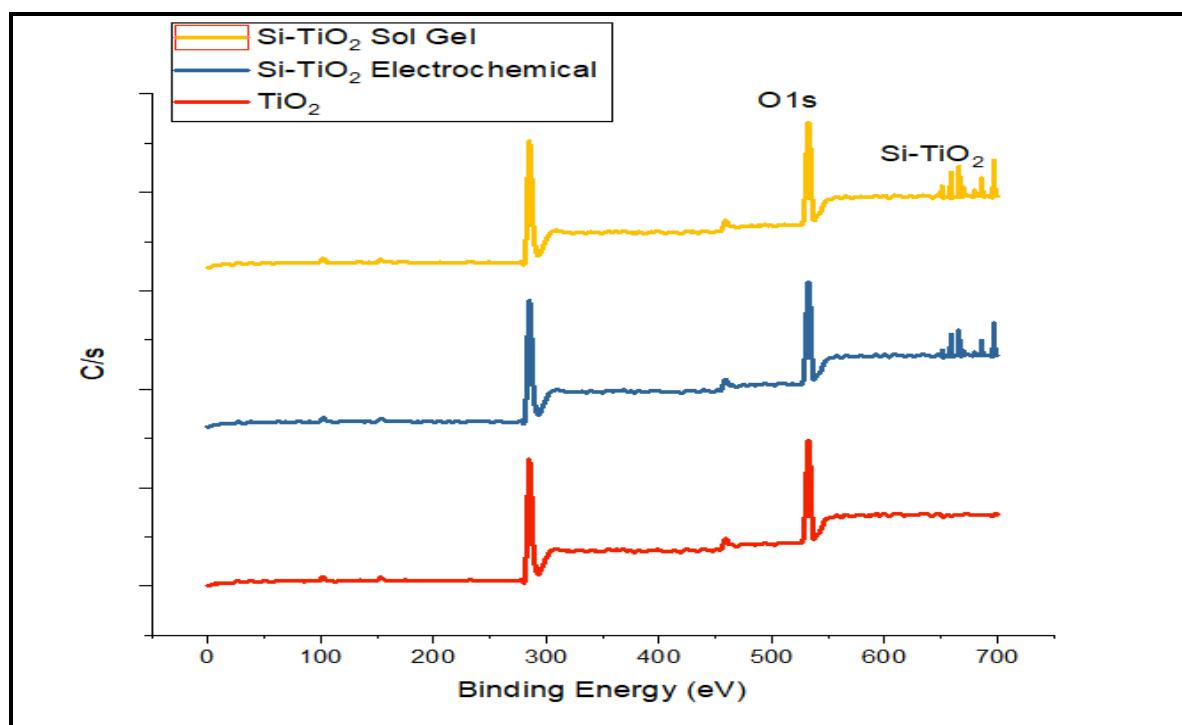
**Figure 5** XRD spectra of MPSi–TiO<sub>2</sub> composites obtained by sol–gel and electrochemical methods

Figure 6 shows the full XPS spectra of the MPSi–TiO<sub>2</sub> composites prepared using the sol–gel and electrochemical methods. C, Ti, and O can be clearly identified in both composites. However, a less intense Si–TiO<sub>2</sub> peak was observed in the composite prepared using electrochemical method due to the low TiO<sub>2</sub> amount etched on the surface of the silicon wafer. This result is consistent with the earlier SEM images of the composites surfaces.



**Figure 6** XPS spectra of MPSi–TiO<sub>2</sub> composites using sol–gel and electrochemical methods.

The experiment on photocatalytic activity of the prepared composites with different immobilizing methods was carried out based on our previous work [4]. In short, the solution of methylene blue was placed in a beaker containing the catalyst (the catalyst was placed vertically in the beaker). The light exposure surface of the catalyst was fixed in all runs at 4 cm<sup>2</sup>. In the experiments for commercial TiO<sub>2</sub> (P25), 0.5 g of the catalyst was added to the solution.

The methylene blue degradation kinetics of TiO<sub>2</sub> under steady-state light illumination with the presence of oxygen followed the Langmuir–Hinshelwood (LH) kinetic model. The organic substrates are presumed to be preadsorbed on the photocatalyst surface prior to illumination. The photocatalytic reaction rate depends on the organic contaminant concentration and can be described by the following rate law [4]:

$$\text{rate} = -\frac{dC}{dt} = \frac{kKC}{1+KC} \quad (3)$$

where  $C$  is the organic substrate concentration (mg/L),  $k$  is the first-order rate constant,  $K$  is the adsorption constant of the organic substrate on the photocatalyst, and  $t$  is the illumination time. The above equation is simplified to a pseudo-first-order equation by considering  $KC$  term  $\ll 1$  as follows:

$$\ln\left(\frac{C}{C_0}\right) = -kKt = k_{obs}t \quad (4)$$

Where  $k_{obs}$  is the rate constant of the first-order photodegradation reaction. The observed constant for the photocatalytic first order degradation of MB on the surface of the catalyst was calculated using the plot of  $-\ln(C/C_0)$  versus the irradiation time.

Figure 7 depicts the degradation efficiency of commercial  $\text{TiO}_2$  and MPSi- $\text{TiO}_2$  prepared using sol-gel and electrochemical methods. The dye removal rate was enhanced after the immobilization of  $\text{TiO}_2$  on the surface of the silicon wafer. The enhancement is due to the ability of the modified silicon to assist in the capture of electrons. Figure 7 shows that the performance of commercial titanium oxide was lower than that of the modified catalyst. The dye removal mechanism perfectly fitted the pseudo-first-order kinetic model. Because the photogenerated electron-hole pair recombination is so rapid, interfacial electron transfer is kinetically competitive only when the relevant donor or acceptor is preadsorbed before photolysis. Therefore, MPSi greatly increased the kinetic reactivity of  $\text{TiO}_2$  for MB degradation. The optimum photocatalyst activity was observed with the catalyst prepared using the electrochemical method due to the high porosity obtained using this method, i.e., more active sites. In contrast, the composite prepared using the sol-gel method showed lower activity compared to that of the electrochemical method, even though higher percentage of  $\text{TiO}_2$  was achieved using sol-gel method. This is due to the low adherence of  $\text{TiO}_2$  to the surface of the silicon and lower porosity when using sol-gel method to prepare the catalyst. The photocatalytic activity and reaction rate reduced in the composite prepared using the sol-gel method as a result of the uniform distribution of the catalyst on the surface of the MPSi.

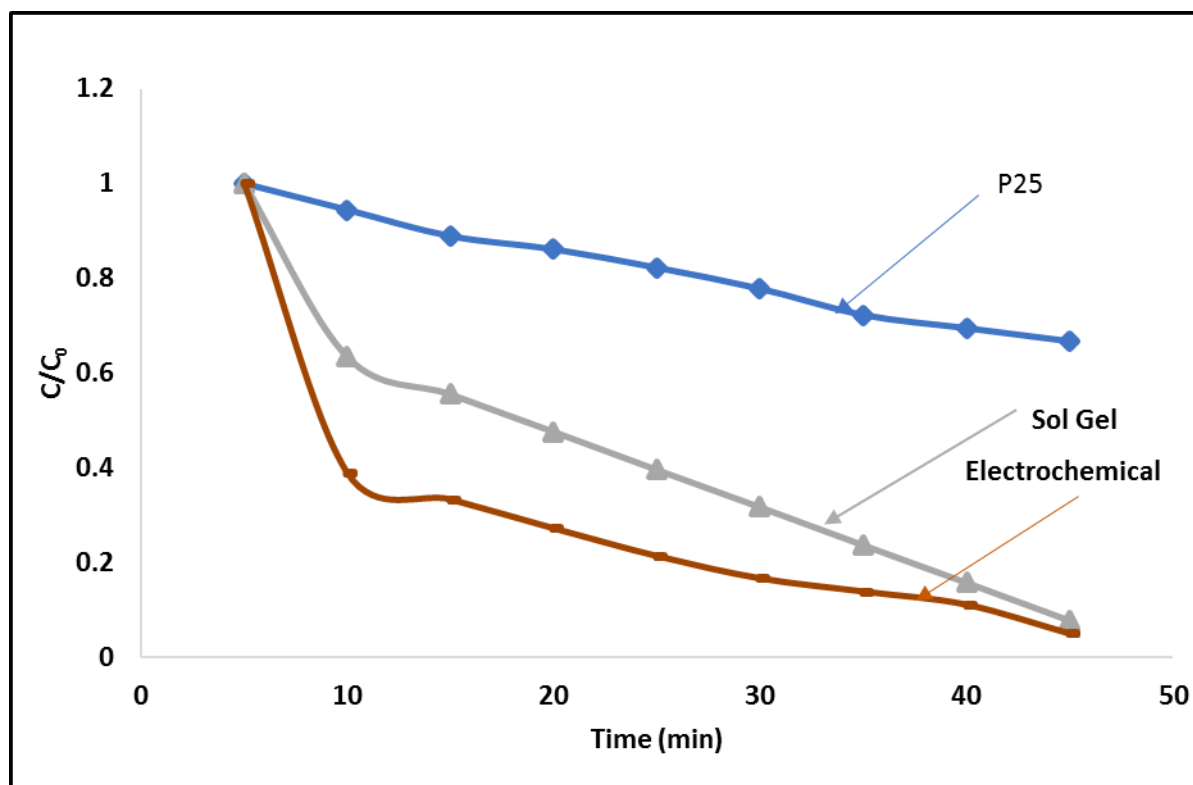


**Figure 7** Photocatalytic degradation of MB with using  $\text{TiO}_2$  and MPSi- $\text{TiO}_2$  composites prepared using sol-gel and electrochemical methods under visible light irradiation.

The MB degradation rate constants ( $k_{\text{obs}}$ ) of the different catalysts were calculated to evaluate their photocatalytic activity and to check the applicability of the LH model. The relation between  $-\ln(C/C_0)$ , where  $C$  and  $C_0$  are the final and initial concentrations of MB, respectively, and the irradiation time ( $t$ ) results was observed to be linear ( $R^2 > 0.92$ ) (Table 2). The slope of this straight line represents  $k_{\text{obs}}$ . The experimental data fitted the pseudo-first-order kinetic model, as shown in Figure 8. The calculated  $k$  values were then used in the basic reaction rate (Equation 3) to calculate the average reaction rate for each catalyst. The average rate is given by the change in concentration,

$\Delta[\text{MB}]$ , divided by the corresponding change in time,  $\Delta t$ . The photocatalytic degradation reaction rate increased when the calcination temperature of the catalyst was increased due to the continuous production of  $\bullet\text{OH}$  radicals during the reaction resulted from the increased photoactivity of the catalyst. The apparent rate constant for MB degradation on the MPSi–TiO<sub>2</sub> composites was higher than that on TiO<sub>2</sub>, as shown in Figure 6 and Table 2. This can be attributed to the surface effects of MPSi, which absorbs part of the incident solar light and acts as an electron sink, resulting in the utilization of more light energy. The experimental results show that  $k_{\text{obs}}$  was higher when using the composite prepared using the electrochemical deposition method. This is consistent with what previously reported for the degradation of MB (Figure 7). The adsorbed MB molecules diffuse to the active sites on the TiO<sub>2</sub> surface and the active sites are responsible for the production of active radicals. Hence, the ratio of  $\bullet\text{OH}$  radicals produced to that consumed increases with an increase in MB adsorption, leading to a faster photodegradation rate. This indicates that the reaction of MB with the  $\bullet\text{OH}$  radicals is the rate limiting step since the adsorption step is faster with MPSi. Additionally, the rate constant for the degradation of MB by MPSi–TiO<sub>2</sub> using electrochemical method is two times higher than that for the commercial TiO<sub>2</sub> with the same absorbed energy, exposed surface area, and initial MB concentration of 18 mg/L.

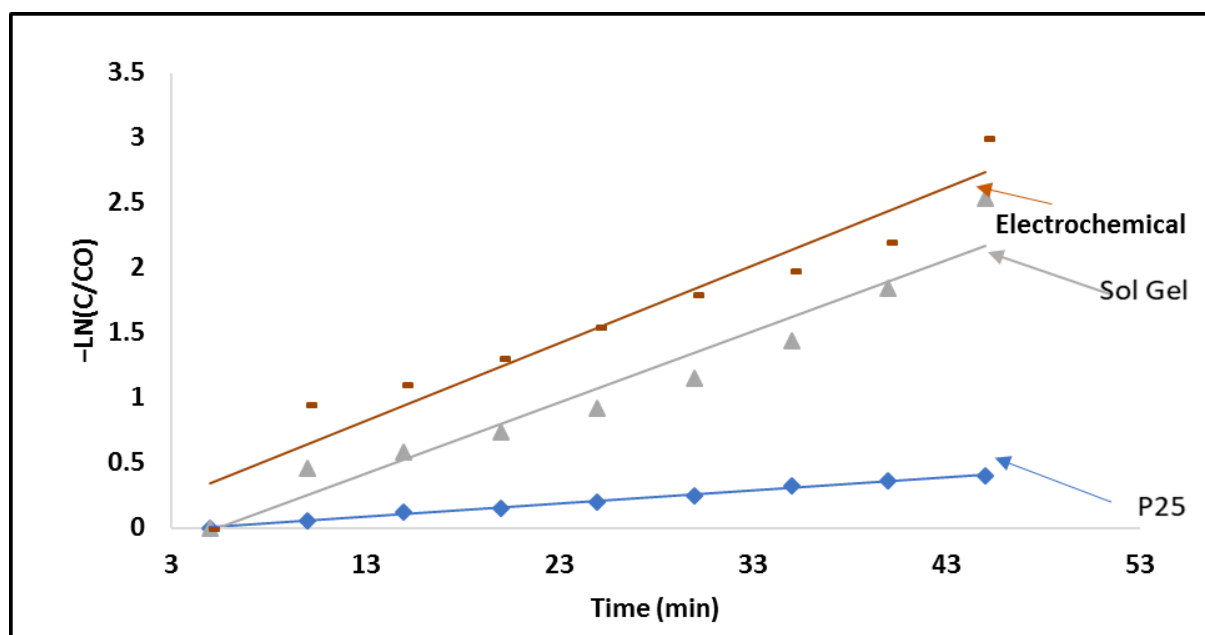


**Figure 8** Degradation kinetics of methylene blue using TiO<sub>2</sub> and MPSi–TiO<sub>2</sub> composites prepared by sol–gel and electrochemical methods under visible light irradiation.

**Table 2** Reaction rate and reaction kinetic constant values of the MPSi–TiO<sub>2</sub> composites.

Catalyst	P25	Sol–gel	Electrochemical
Rate (mg/L·min)	0.0132	0.0207	0.0267
$k_{\text{obs}}$ (min <sup>-1</sup> )	0.009	0.0205	0.0279
$R^2$	0.9962	0.9653	0.933

#### 4. Conclusions

MPSi–TiO<sub>2</sub> composites were prepared through electrochemical immobilization of titanium dioxide on silicon surface. The MPSi–TiO<sub>2</sub> composites can be used as photocatalysts under ambient conditions and visible light to degrade organic contaminants. The results show that the MPSi–TiO<sub>2</sub> composites exhibited a much higher stability and activity than bare TiO<sub>2</sub>. The microscopic analysis of the produced composites showed a better uniform distribution of TiO<sub>2</sub> on the surface of MPSi produced using the electrochemical deposition compared to the conventional immobilization method (sol–gel method). In contrast, the thickness of the TiO<sub>2</sub> film on the surface of MPSi was larger in the composite produced using the sol–gel method which was confirmed by the EDX analysis. This is due to the advantage of sol–gel method where controlling the immobilized layer thickness in the sol-gel method by the appropriate changes of coating variables. In the context of photoactivity, electrochemical deposition method produced a composite with better performance even at low TiO<sub>2</sub> content due to the strong adherent between TiO<sub>2</sub> and MPSi surface. It can be concluded that the immobilization of TiO<sub>2</sub> by the electrochemical method can lead to the fabrication of catalysts with better photocatalytic activity compared to the conventional methods.

#### Acknowledgement

The research is financially supported by the universiti Malaysia Pahang under the grant (RDU 1603152). Authors are greatly thankful to CARIFF center for facilitating the research.

#### References

- [1] Ruokolainen M, Ollikainen E, Sikanen T, Kotiaho T and Kostianen R 2016 Oxidation of Tyrosine-Phosphopeptides by Titanium Dioxide Photocatalysis *J. Am. Chem. Soc.* **138** 7452-5
- [2] Fujishima A, Rao T N and Tryk D A 2000 Titanium dioxide photocatalysis *J. photochem. photobio. C: Photochem. rev.* **1** 1-21
- [3] Fujishima A and Zhang X 2006 Titanium dioxide photocatalysis: present situation and future approaches *CR CHIM* **9** 750-60
- [4] Basheer E A and Abdulbari H A 2018 Visible Light TiO<sub>2</sub> Photocatalyst Composite Based on Carbon Microfiber Derived from Human Hair *ChemistrySelect* **3** 11687-95
- [5] Carp O, Huisman C L and Reller A 2004 Photoinduced reactivity of titanium dioxide *J. Solid State Chem.* **32** 33-177
- [6] Yuan R-S, Zheng J-T, Guan R-B and Liu Y-H 2005 Immobilization of TiO<sub>2</sub> on microporous activated carbon fibers and their photodegradation performance for phenol *New Carbon Materials* **20** 45-50
- [7] Serpone N 2006 Is the band gap of pristine TiO<sub>2</sub> narrowed by anion-and cation-doping of titanium dioxide in second-generation photocatalysts? : ACS Publications)
- [8] Asahi R, Morikawa T, Ohwaki T, Aoki K and Taga Y 2001 Visible-light photocatalysis in nitrogen-doped titanium oxides *science* **293** 269-71
- [9] Phattalung S N, Limpijumnong S and Yu J 2017 Passivated co-doping approach to bandgap narrowing of titanium dioxide with enhanced photocatalytic activity *Appl Catal B-Environ* **200** 1-9
- [10] Jin M, Nagaoka Y, Nishi K, Ogawa K, Nagahata S, Horikawa T, Katoh M, Tomida T and Hayashi J i 2008 Adsorption properties and photocatalytic activity of TiO<sub>2</sub> and La-doped TiO<sub>2</sub> *Adsorption* **14** 257-63
- [11] Bahrudin N N and Nawi M A 2018 Immobilized titanium dioxide/powdered activated carbon system for the photocatalytic adsorptive removal of phenol *Korean J Chem Eng* 1-10

- [12] Zheng X, Yu N, Wang X, Wang Y, Wang L, Li X and Hu X 2018 Adsorption Properties of Granular Activated Carbon-Supported Titanium Dioxide Particles for Dyes and Copper Ions *Sci. Rep.* **8**
- [13] Orha C, Pode R, Manea F, Lazau C and Bandas C 2017 Titanium dioxide-modified activated carbon for advanced drinking water treatment *Process. Saf. Environ.* **108** 26-33
- [14] Atchudan R, Edison T N J I, Perumal S, Karthikeyan D and Lee Y R 2017 Effective photocatalytic degradation of anthropogenic dyes using graphene oxide grafting titanium dioxide nanoparticles under UV-light irradiation *J. Photoch. Photobio. A* **333** 92-104
- [15] Suave J, Amorim S M, Ângelo J, Andrade L, Mendes A and Moreira R F 2017 TiO<sub>2</sub>/reduced graphene oxide composites for photocatalytic degradation in aqueous and gaseous medium *J. Photoch. Photobio. A* **348** 326-36
- [16] Kuo H-P, Yao S-W, Huang A-N and Hsu W-Y 2017 Photocatalytic degradation of toluene in a staged fluidized bed reactor using TiO<sub>2</sub>/silica gel *Korean. J. Chem. Eng.* **34** 73-80
- [17] Seo H O, Kim D H, Kim K-D, Park E J, Sim C W and Kim Y D 2013 Adsorption and desorption of toluene on nanoporous TiO<sub>2</sub>/SiO<sub>2</sub> prepared by atomic layer deposition (ALD): influence of TiO<sub>2</sub> thin film thickness and humidity *Adsorption* **19** 1181-7
- [18] López T, Alvarez M, González R, Uddin M, Bustos J, Arroyo S and Sánchez A 2011 Synthesis, characterization and in vitro cytotoxicity of Pt-TiO<sub>2</sub> nanoparticles *Adsorption* **17** 573-81
- [19] Lee D H, Cho Y S, Yi W I, Kim T S, Lee J K and Jin Jung H 1995 Metalorganic chemical vapor deposition of TiO<sub>2</sub>: N anatase thin film on Si substrate *Appl. phy. letters* **66** 815-6
- [20] Puma G L, Bono A, Krishnaiah D and Collin J G 2008 Preparation of titanium dioxide photocatalyst loaded onto activated carbon support using chemical vapor deposition: A review paper *J. Hazard. Mater.* **157** 209-19
- [21] Al-Jawad S M 2017 Structural and optical properties of core-shell TiO<sub>2</sub>/CdS prepared by chemical bath deposition *J. Electron. Mater.* **46** 5837-47
- [22] Duenas S, Castán H, García H, San Andrés E, Toledano-Luque M, Mártel I, González-Díaz G, Kukli K, Uustare T and Aarik J 2005 A comparative study of the electrical properties of TiO<sub>2</sub> films grown by high-pressure reactive sputtering and atomic layer deposition *Semicond. Sci. Tech.* **20** 1044
- [23] Pei C C and Leung W W-F 2013 Photocatalytic degradation of Rhodamine B by TiO<sub>2</sub>/ZnO nanofibers under visible-light irradiation *Separation and purification technology* **114** 108-16
- [24] Santos A and Kumeria T 2015 *Electrochem. Eng. Nanoporous Mater.:* Springer) pp 1-36